J. Embryol. exp. Morph. **80**, 21–41 (1984)
Printed in Great Britain © *The Company of Biologists Limited 1984*

Development of the apical ectodermal ridge in the chick wing bud

By WILLIAM L. TODT AND JOHN F. FALLON[1]

Department of Anatomy, The University of Wisconsin, Madison, Wisconsin 53706, U.S.A.

SUMMARY

Histological examination of the stage-18 to stage-23 chick wing bud apex revealed the following. Initially, the wing bud was covered by a cuboidal to columnar epithelium with an overlying periderm. Thickening of the apical ectoderm was not obvious until late stage 18 (36 pairs of somites), after the appearance of the wing bud. At late stage 18, cells of the inner layer of ectoderm had elongated slightly along an axis perpendicular to the epithelial-mesenchymal interface. Well-defined apical ectodermal ridge morphology, i.e., pseudostratified columnar epithelium with an overlying periderm, was not apparent until stage 20. Subsequently the ridge lengthened along the anteroposterior perimeter of the wing bud. We demonstrated histologically that the apical ectodermal ridge of the wing bud was asymmetric with respect to the anteroposterior axis, in that there was more ridge associated with posterior mesoderm. Other observations include the spatial and temporal location of a groove in the base of the thickest part of the ridge. The groove can be correlated with the specification of distal wing elements. The groove was first seen at stage 20 and became more prominent through stage 23. An anteroposterior progression of ectodermal cell death was also observed. This began at late stage 18 and continued through each of the stages examined.

INTRODUCTION

The development of the limb bud of the chick embryo is dependent upon a series of interactions between the limb bud mesoderm and overlying ectoderm. The mesoderm induces the formation of a pseudostratified columnar epithelium at the apex of the bud (Kieny, 1968; Saunders & Reuss, 1974) which is called the apical ectodermal ridge (Saunders, 1948). The ridge is distinct from the simple cuboidal epithelium of the dorsal and ventral limb bud surfaces (Ede, Bellairs & Bancroft, 1974; Fallon & Kelley, 1977). Removal of the ridge results in limbs with predictable terminal deficiencies. The longer the mesoderm is associated with the ridge, the more distally complete the resultant limb will be (Saunders, 1948; Summerbell, 1974; Rowe & Fallon, 1982). Thus, the ridge may be viewed as an inducer of normal avian limb bud outgrowth (Saunders, 1977).

In a previous systematic study of the chick wing bud, Jurand (1965) presented representative sections of the wing bud apex from stages 16 to 31. Sections were selected and interpreted from serially sectioned material embedded in paraffin.

[1] For reprint requests.

This work constitutes the most informative description of ridge development to date. However, there are limitations inherent in the use of paraffin embedded material. These include the inability to control the orientation of the tissue when it is sectioned and difficulty in interpreting the position of the sections relative to the tissue as a whole. To facilitate further morphological and experimental studies on the development and function of the apical ectodermal ridge, we have done a systematic study of ridge development using electron microscopic fixation procedures and plastic embedment. The results of this study are the subject of this report.

MATERIALS AND METHODS

Fixation and embedment

Standard techniques were used to obtain stage-18 to -23 White Leghorn embryos (Hamburger & Hamilton, 1951). Embryos were fixed in a solution of formaldehyde (2 %), glutaraldehyde (2·5 %), and picric acid (0·02 %), buffered with 0·075 M-phosphate buffer, pH 7·3 (Fallon & Kelley, 1977). They were then lightly postfixed in osmium tetroxide to facilitate counting of the somites and visualization of the tissue. Wing buds and adjacent tissues were embedded flat in epon. The tissue was placed with the dorsal wing bud surface just beneath the surface of the block to allow clear visualization of the tissue. Both wing buds from at least one embryo at each stage were examined. The data from right and left wing buds from the same embryo were in agreement.

Sectioning

Camera-lucida drawings were made of embedded tissue (e.g., Fig. 1B), paying special attention to the outline of the wing bud, the adjacent somites (stages 18 to 20) and the anterior and posterior junctions of the wing bud and body wall (stages 20 to 23). To obtain accurate measurements of ectodermal thickness, it was necessary that the sections be cut in the dorsoventral plane perpendicular to the apical epithelium (cross sections). At each location, three adjacent sections were cut, 1 to 1·5 μm thick. To insure that cross sections were in fact cut, the block was then realigned with the camera-lucida drawing and the position (location and orientation) of the face of the block was recorded on the drawing. In addition to recording the position of the sections, it was possible to predict the change in orientation of the block needed to remain perpendicular to the apical epithelium of the bud for cutting the next group of cross sections. By repeating the procedure of cutting and marking, cross sections from 20 to 40 different locations along the apex of each bud were obtained. Sections were stained with azure II-methylene blue (0·5 %).

Determination of location of sections

For stages 18 to 20, the location of the cross sections could be expressed with reference to the adjacent somites. At later stages, when reference to the somites

was difficult, the location was expressed relative to the distance along the anteroposterior perimeter of the wing bud. The anteroposterior perimeter was defined as the outline of the wing bud from the anterior to posterior junction of the bud and body wall, as seen by viewing the dorsal surface of the wing bud. Thus, 0 % and 100 % of the anteroposterior perimeter represented the anterior and posterior junctions of the wing bud and body wall, respectively (see Figs 4A and 4B). Stage 20 was a transition between the two methods as values relative to both the perimeter and the somites could be assigned to each location (see Fig. 4A).

As wing outgrowth continues, the wing level somites increase in size and the anteroposterior perimeter increases in length (compare Figs 4B and 8B). Therefore, it is stressed that direct comparison of graphs from different stages may be deceptive. It should be noted also that 50 % of the anteroposterior perimeter did not necessarily correspond to the theoretical anteroposterior midline (axial line; see Figs 4A, 6A and 8A).

Determination of ectodermal thickness

A filar micrometer was used to measure ectodermal thickness for the three sections at each location. These measurements were made along a line which passed through the thickest portion of the apical ectoderm (including periderm) and was normal to the line tangential to the base of the ectoderm. The ectodermal thickness for each location was calculated by averaging these measurements. Because of the possibility that the plane of section was not always exactly perpendicular to the apical epithelium, the average thickness was corrected for this potential problem. A correction factor was calculated taking into account, 1) the rate of change in ectodermal thickness in a given region, as determined from the raw data, and 2) the orientation of the plane of section with respect to the line perpendicular to the outline of the wing bud at that location, as measured on the camera-lucida drawing.

To keep the magnitude of these corrections in perspective, we point out that only 1·8 % (15 of 834) of the locations examined had a correction greater than 2·0 %. Only 2 of these 15 corrections were larger than 5 %, viz., 6·6 % and 7·3 %. It is equally important to note that measurements from adjacent sections at the same location could show variation of 2 %, probably due to the unevenness of the outer peridermal surface (cf. Camosso & Roncali, 1968). Thus, while the magnitude of the correction did not significantly alter the data presented in this report, it was utilized for consistency.

RESULTS

Data for some of the epithelial characteristics described in this section are summarized in Table 1.

Table 1. *Summary of wing bud apical epithelial characteristics*

Stage (Pairs of somites)	No. examined	Thickest ectoderm (μm)	Limits of ectodermal cell death	Contour of ectodermal base
18 (32–33)	6	20	no cell death	smooth
18+ (36)	5	24–30	somites 15–17	smooth
19 (38)	5	30–35	mid somite 16 – mid somite 18	smooth
20 (41–42)	7	38–44	somites 16–18 (0% to 60% of perimeter)	slight notch
21	5	37–45	20% to 60% of perimeter	notch
23	5	33–38	20% to 83% of perimeter	notch

Stage 18 (32–33 pairs of somites, Table 1 and Fig. 1)

The wing bud ectoderm at this early stage consisted of irregular cuboidal to columnar cells with an overlying simple squamous periderm. Five wing buds were examined at the level of somite 15 (Figs 1A, B), and in three of these a thickening was seen at this level. The thickening was localized ventrally and was not considered a ridge, as no prominence was seen in the outline of the outer ectodermal surface (Figs 1A, B, C). The apical ectoderm around the level of the

Fig. 1. Stage 18 (32–33 pairs of somites).

(A) The relationship between ectodermal thickness and location (relative to somite level) for six wing buds. Solid dots are data from the wing bud pictured in (B). Letters along the abscissa correspond to locations in (B) and to micrographs (C) through (H). It is crucial to point out that the graph does not represent the outline of the wing bud, but the change in ectodermal thickness along the anteroposterior extent of the wing bud. This cautionary note also applies to Figs 2A, 3A, 4A, 6A and 8A.

(B) Camera-lucida drawing of the wing bud indicated by solid dots in (A). Somites are numbered at the left and the curve indicated by the arrows is the outline of the wing bud. Lines intersecting the wing bud outline show the position of sections examined for that wing bud. Heavy lines have letters corresponding to those along the abscissa in (A) and to micrographs (C) through (H). Scale bars (A and B) represent 250 μm.

(C) through (H) Micrographs of cross sections of the wing bud at positions indicated by the corresponding letters in (B). The micrographs are oriented with distal mesoderm covered by apical ectoderm. Dorsal is to the left, ventral to the right. Note the anterior thickening (C, arrows). Anterior ectoderm is thicker than posterior ectoderm (compare D and G). No ectodermal cell death is seen. Scale bar (C) represents 20 μm.

junction of somites 17 and 18 was 17 to 20 μm thick. Intercellular spaces were generally smaller than those in adjacent dorsal and ventral ectoderm, and suggestions of nuclear stratification were apparent (e.g., Figs 1D to 1F). Posteriorly, there was a decrease in apical ectodermal thickness so that at the level of the junction of somites 20 and 21, it was 9 to 15 μm thick (Figs 1A, H). Ectodermal cell death was not observed at this stage.

Late stage 18 (36 pairs of somites, Table 1 and Fig. 2)

At the level of somite 15 (Figs 2A, B), a thickening of ectoderm was seen on the ventral surface of the wing bud (Figs 2A, B, C), near the lateral body fold (Hamburger & Hamilton, 1951). Around the level of somite 18, the apical epithelium was thickened to at least 24 μm. From examination of cross sections

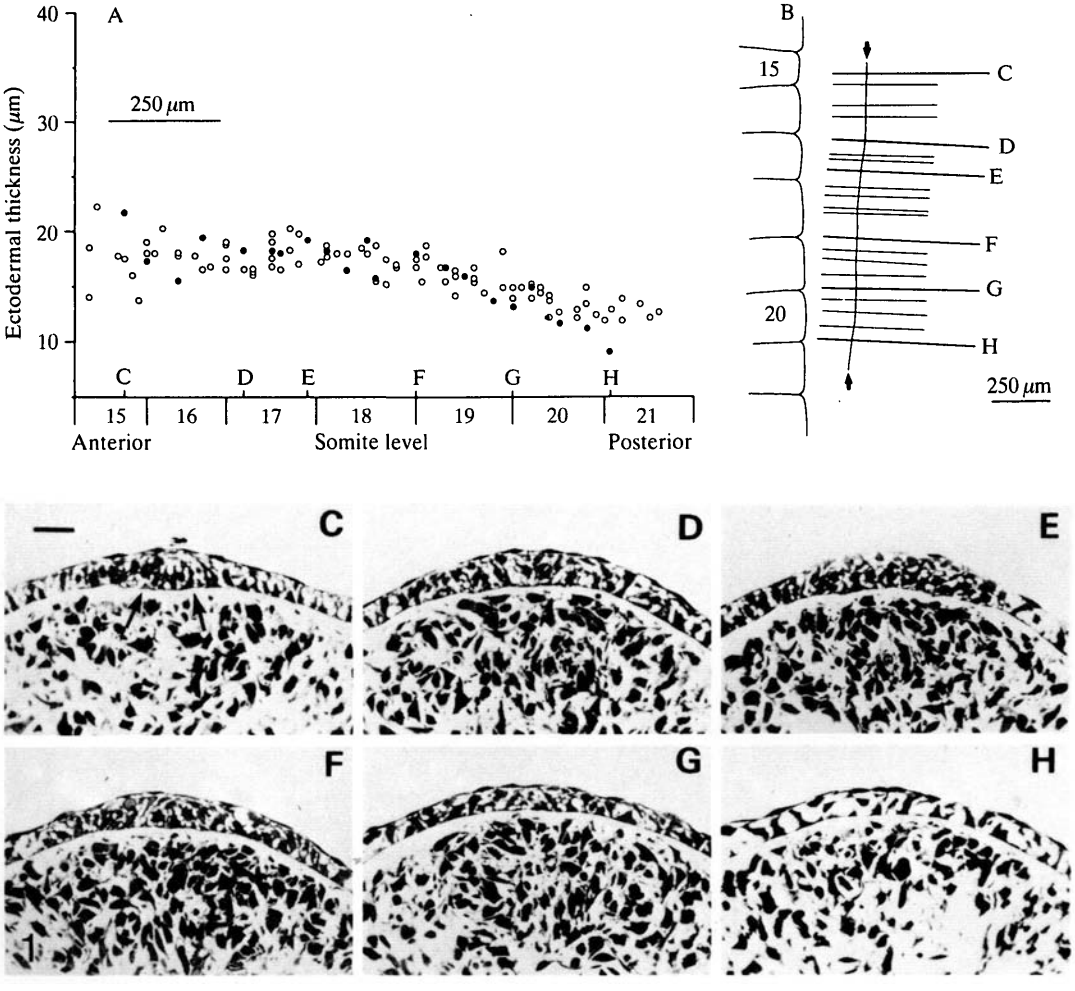

Fig. 1

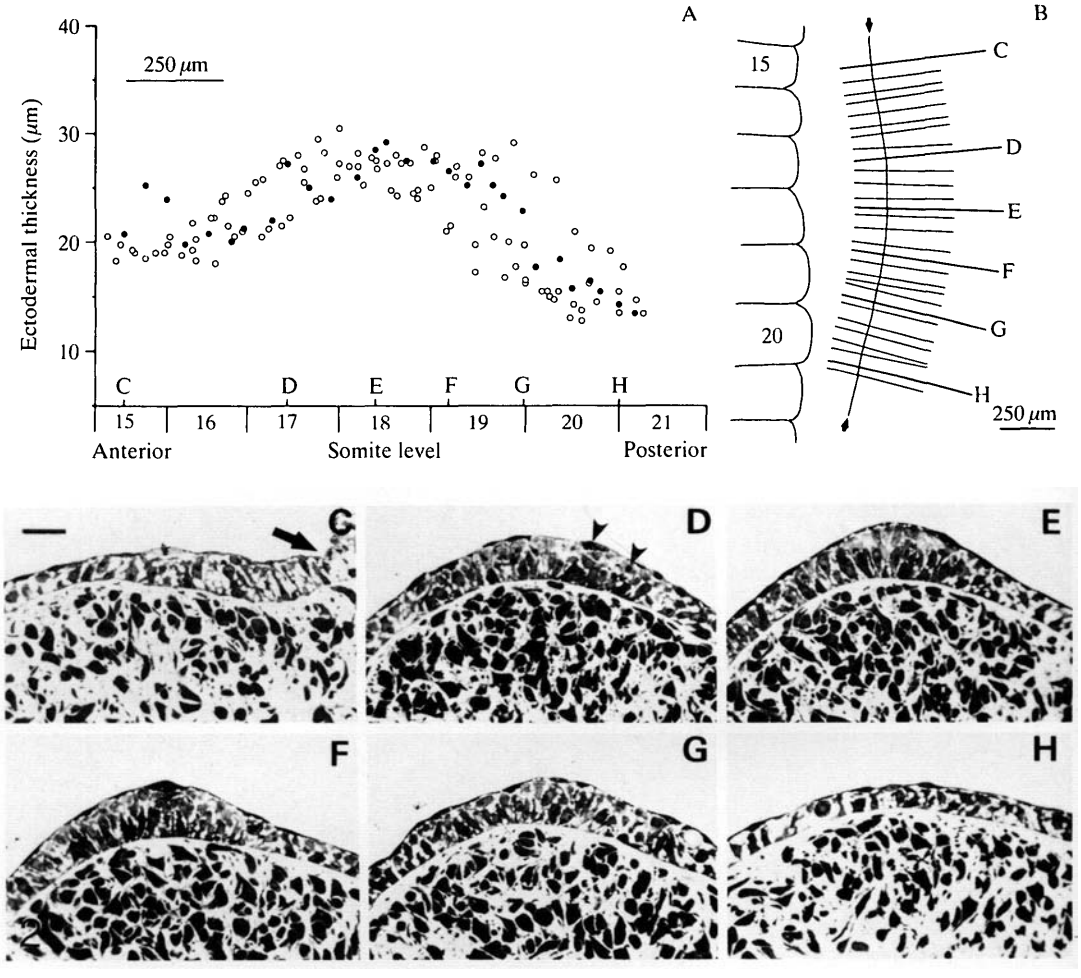

Fig. 2. Late stage 18 (36 pairs of somites).

(A) The relationship between ectodermal thickness and location (relative to somite level) for five wing buds. Solid dots are data from wing bud pictured in (B). Letters along the abscissa correspond to locations in (B) and to micrographs (C) through (H).

(B) Camera-lucida drawing of the wing bud indicated by solid dots in (A). Somites are numbered at the left and the curve indicated by the arrows is the outline of the wing bud. Lines intersecting the wing bud outline show the position of sections examined for that wing bud. Heavy lines have letters corresponding to those along the abscissa in (A) and to micrographs (C) through (H). Scale bars (A and B) represent 250 μm.

(C) through (H) Micrographs of cross sections of the wing bud at positions indicated by the corresponding letters in (B). Micrographs are oriented with distal mesoderm covered by apical ectoderm. Dorsal is to the left, ventral to the right. Note the anterior thickening (C) very close to the lateral body fold (arrow). Cell death is seen in some anterior apical ectoderm (D, arrowheads). Dorsoventral asymmetry is seen clearly in (F). Scale bar (C) represents 20 μm.

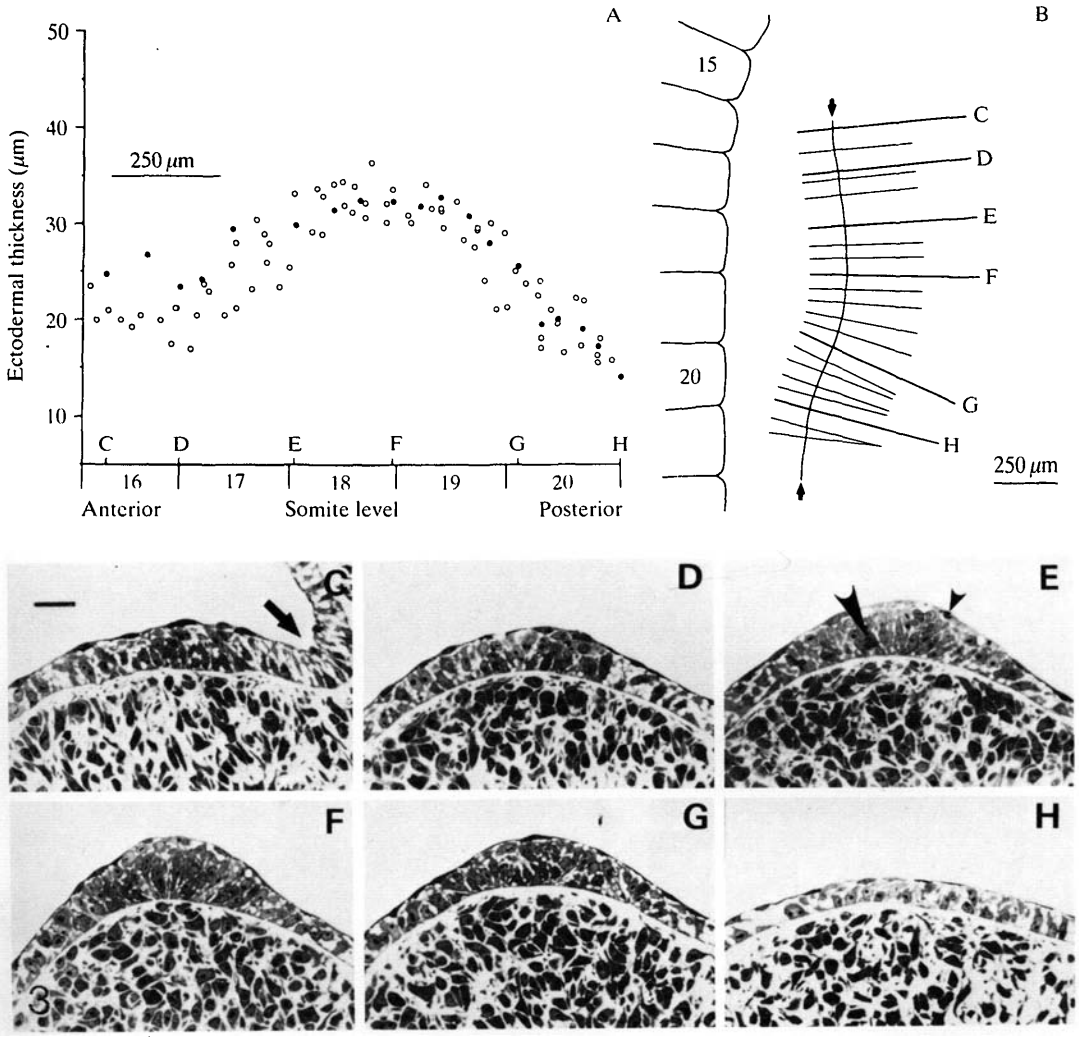

Fig. 3. Stage 19 (38 pairs of somites).

(A) The relationship between ectodermal thickness and location (relative to somite level) for five wing buds. Solid dots are data from wing bud pictured in (B). Letters along the abscissa correspond to locations in (B) and to micrographs (C) through (H).

(B) Camera-lucida drawing of the wing bud indicated by solid dots in (A). Somites are numbered at the left and the curve indicated by the arrows is the outline of the wing bud. Lines intersecting the wing bud outline show the position of sections examined for that wing bud. Heavy lines have letters corresponding to those along the abscissa in (A) and to micrographs (C) through (H). Scale bars (A and B) represent 250 μm.

(C) through (H) Micrographs of cross-sections of the wing bud at positions indicated by the corresponding letters in (B). Micrographs are oriented with distal mesoderm covered by apical ectoderm. Dorsal is to the left, ventral to the right. Note the anterior ectodermal thickening (C) very close to the lateral body fold (arrow) and the ectodermal cell death (E, arrowheads). Obvious dorsoventral asymmetry is seen in (F). Scale bar (C) represents 20 μm.

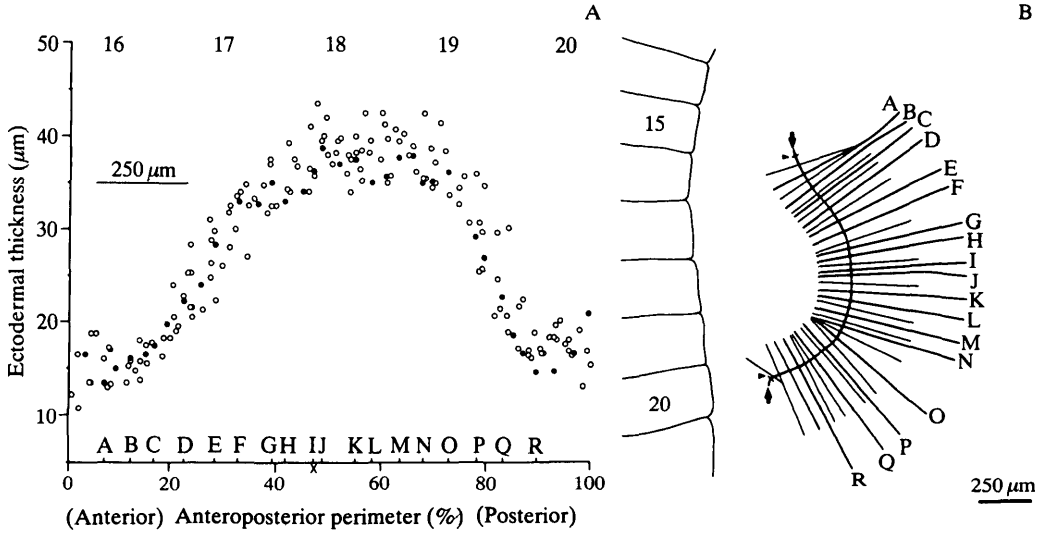

Fig. 4. Stage 20 (41–42 pairs of somites).

(A) The relationship between ectodermal thickness and location (relative to the anteroposterior perimeter) for seven wing buds. Approximate somite levels are indicated across the top. Solid dots are data from wing bud pictured in (B). Letters along the abscissa correspond to locations in (B) and to the micrographs in Fig. 5. To determine the position of the axial line, indicated by the X (47·5 % ± 0·9 S.D.), a line representing the base of the wing bud was drawn by connecting the anterior and posterior junctions of the bud and the body wall (see Fig. 4B). The axial line was drawn perpendicular to the base of the bud, midway between the anterior and posterior junctions of the bud and the body wall.

(B) Camera-lucida drawing of the wing bud indicated by the solid dots in (A). The curve indicated by the arrows is the outline of the wing bud; the anterior and posterior boundaries of the wing bud are indicated by the arrowheads. Lines intersecting the wing bud outline mark the position of the sections examined for that wing bud. Heavy lines have letters corresponding to those along the abscissa in (A) and to the micrographs in Fig. 5. Scale bars (A and B) represent 250 μm.

Fig. 5. Stage 20 (41–42 pairs of somites). Micrographs of cross sections of the wing bud at the locations indicated by the corresponding letters in Fig. 4B. Distal mesoderm is covered with apical ectoderm. Dorsal is to the left, ventral to the right. Micrographs are lettered in sequence, (A) being the most anterior (cranial). In addition, the micrographs are paired. For example, (A) and (R) are approximately the same distance from the axial line, as are (B) and (Q), etc. Note the apical ectodermal cell death (A through F, see arrowheads) and dorsoventral asymmetry (e.g., I through K). Compare the subectodermal region in (A) and (R). In addition, a slight notch is evident in the base of the ectoderm of some sections (see arrow, L). Anteroposterior asymmetry of the entire ridge with respect to the axial line is apparent when comparing (A) through (D) with (O) through (R). Scale bar (A) represents 20 μm.

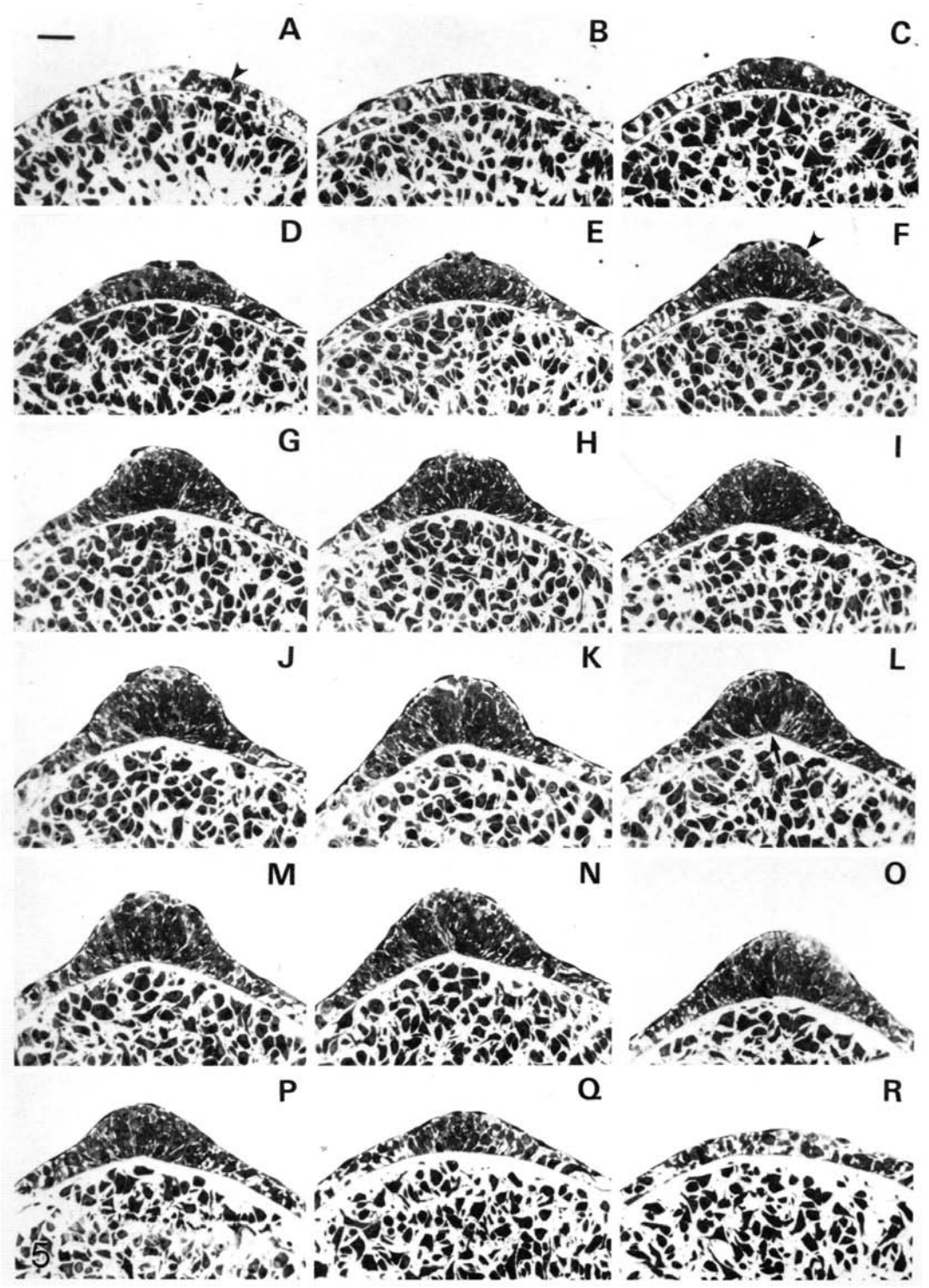

Fig. 5

between these two regions, it was seen that the thickenings were continuous. In the region opposite somite 18, the ectoderm comprised elongated cells which were often radially arranged (Fig. 2E). In most of the cross sections (43 of 56) in this region, an obvious dorsoventral asymmetry was seen in that the transition from apical to ventral ectoderm was more pronounced than the transition from apical to dorsal ectoderm. In addition, the thickest ectoderm was located slightly ventral with respect to the apex of the mesodermal core as seen in cross sections (Fig. 2F; cf., Zwilling, 1961). The intercellular spaces were smaller than those seen at the previous stage. Apical ectoderm at the level of the junction of somites 20 and 21 was similar to adjacent dorsal and ventral ectoderm (12 to 18 μm, Fig. 2H).

The occurrence of an average of two necrotic loci in each cross section of the apical ectoderm at a given location was considered evidence of cell death. Ectodermal cell death was evident in all wing buds at this stage and was limited to anterior ectoderm opposite somites 15 through 17 (Fig. 2D). The precise distribution within this region varied from bud to bud. However, it should be noted that cell death in the apical ectoderm was not seen posterior to the level of the middle third of somite 17.

Stage 19 (38 pairs of somites, Table 1 and Fig. 3)

In three wing buds examined at the level of somite 16 (Figs 3A, B), a thickening was seen in the ventral ectoderm near the lateral body fold (Figs 3A, B, C). As seen in the previous stage, the thickening was continuous with the thickening of the apical epithelium of more posterior wing bud levels (Figs 3C, D, E). The apical ectoderm at the level of the caudal 2/3 of somite 18 and the cranial 2/3 of somite 19 was consistently thicker than 27 μm. The architecture was similar to that of the thickest regions of late stage-18 wing bud ectoderm, but there were fewer and smaller intercellular spaces (compare Figs 2F and 3F). It should be noted that the thickest ridge was in the posterior half of the wing bud around the level of the junction of somites 18 and 19. Posteriorly, the apical ectoderm decreased in thickness to about 15 μm and was similar to adjacent dorsal and ventral ectoderm (Fig. 3H). The base of the ectoderm was smooth at all anteroposterior levels.

Cell death in the ectoderm was seen in only two of the wing buds examined (arrowheads, Fig. 3E). Ectodermal cell death was not seen posterior to the level of the middle of somite 18 in any stage-19 wing bud examined.

Stage 20 (41–42 pairs of somites, Table 1 and Figs 4 and 5)

Anteriorly, at approximately the level of somite 16 (from 0 % to about 15 % of the anteroposterior perimeter, Figs 4A, B; 5A, B), the apical ectoderm was comprised of cuboidal to columnar cells with an overlying periderm and a smoothly contoured base. Suggestions of nuclear stratification were evident in some parts of the ectoderm. There were large intercellular spaces and the

ectodermal thickness ranged from 11 to 19 μm. Continuing posteriorly to the level of the middle of somite 18 (anteroposterior midline, 47 % of the anteroposterior perimeter, Figs 4A, B; 5C to 5I), the apical ectoderm thickened progressively to about 38 μm and acquired the appearance of a pseudostratified columnar epithelium with overlying periderm. Intercellular spaces became smaller and sparser as the cells assumed the radial arrangement typical of thick ridge (e.g., Fig. 5J). The ridge at the level around the junction of somites 18 and 19 (53 % to 65 % of the anteroposterior perimeter, Figs 4A, B; 5K, L, M) consistently showed a slight notch in the base of the epithelium (18 of 21 cross sections; Fig. 5L, arrow). The notch was located near the dorsoventral midline of the ridge and was the point around which the cells of the ridge were radially arranged. Most of the cross sections (59 of 62) that displayed the ectodermal notch were found opposite somites 18 and 19 (from 38 % to 78 % of the anteroposterior perimeter). These cross sections (about 40 % to 70 % of the anteroposterior perimeter) also had the same dorsoventral asymmetry that was seen in the two previous stages (Fig. 5K). The thickness of the ectoderm in this region was 34 to 44 μm. Near the level of the junction of somites 19 and 20 (about 75 % of the anteroposterior perimeter), the ectodermal thickness began to decrease (Figs 5O, P). At the level of the middle of somite 20 (90 % of the anteroposterior perimeter) the ectoderm was 16 to 20 μm thick (Fig. 5R) and was similar in appearance to anterior apical ectoderm. Cell death was seen in the apical ectoderm of all stage-20 wing buds (Figs 5A to 5F). It was not seen posterior to 60 % of the anteroposterior perimeter.

Beginning at stage 20, a difference could be seen when comparing the region immediately subjacent to the ectoderm along the anterior versus posterior border of the wing bud. Along the anterior border, the mesodermal cells were very close to the base of the ectoderm, while along the posterior border there was consistently a narrow region beneath the ectoderm that appeared to be free of cell profiles (compare Figs 5A and 5R).

Stages 21 and 23 (Table 1 and Figs 6 through 9)

In general, the description of the stage-20 apical ectoderm applies to stages 21 and 23 with only minor changes (see Table 1 and Figs 6A and 8A). The following are notable exceptions. The distance along the anteroposterior perimeter increased (compare Figs 4A, B with 6A, B and 8A, B). At anterior levels, cell death of the anterior necrotic zone (Saunders, Gasseling & Saunders, 1962) was seen in the mesoderm of both stages (arrowheads, Figs 7A and 9A). At stage 21 the basal notch was always seen between 40 % and 75 % of the anteroposterior perimeter (Figs 7I to 7P). At stage 23, the notch was evident in all sections between 40 % and 71 % of the anteroposterior perimeter (Figs 9D to 9O). By comparing Figs 5L and 9L, it can be seen that the notch became progressively more prominent between stages 20 and 23. In addition, the transitions from ridge to dorsal and ventral ectoderm were more pronounced than at previous stages. However, the dorsoventral asymmetry of the ridge was not as evident (compare

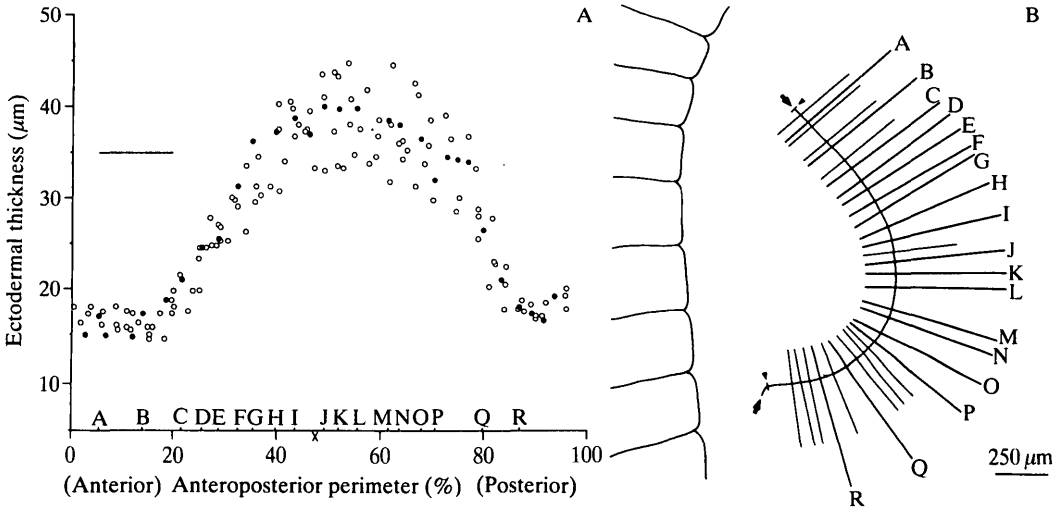

Fig. 6. Stage 21.

(A) The relationship between ectodermal thickness and location (relative to the anteroposterior perimeter) for five wing buds. Solid dots are data from the wing bud pictured in (B). Letters along the abscissa correspond to locations in (B) and to the micrographs in Fig. 7. The position of the axial line (see explanation, Fig. 4A) is indicated by the X (47·6 % ± 1·7 S.D.).

(B) Camera-lucida drawing of the wing bud indicated by the solid dots in (A). The curve indicated by the arrows is the outline of the wing bud; the anterior and posterior boundaries of the wing bud are indicated by the arrowheads. Lines intersecting the wing bud outline mark the position of the sections examined for that wing bud. Heavy lines have letters corresponding to those along the abscissa in (A) and to the micrographs in Fig. 7. Scale bars (A and B) represent 250 μm.

Figs 5 and 9). Cell death was seen in the ectoderm of all wing buds at these stages (see Table 1 and Figs 7C to 7I, and 9C to 9P). By stage 23, the entire portion of thick ectoderm (20 % to 83 % of the anteroposterior perimeter) had cell death associated with it. The same differences in the subectodermal region, observed between the anterior and posterior border of the wing bud at stage 20, were also seen at stages 21 and 23 (compare Figs 7A with 7R, and 9A with 9R).

Fig. 7. Stage 21. Micrographs of cross-sections of the wing bud at the locations indicated by the corresponding letters in Fig. 6B. Distal mesoderm is covered with apical ectoderm. Dorsal is to the left, ventral to the right. Micrographs are lettered in sequence, (A) being the most anterior (cranial). In addition, the micrographs are paired. For example, (A) and (R) are approximately the same distance from the axial line, as are (B) and (Q), etc. Mesodermal cell death (anterior necrotic zone) is seen (A, arrowhead). Note the apical ectodermal cell death (C through I, see arrowheads). Compare the subectodermal region in (A) and (R). At this stage, the notch is more pronounced than at the previous stage (see arrow, J). Anteroposterior asymmetry of the ridge with respect to the axial line is apparent when comparing (D) through (F) with (M) through (O). Scale bar (A) represents 20 μm.

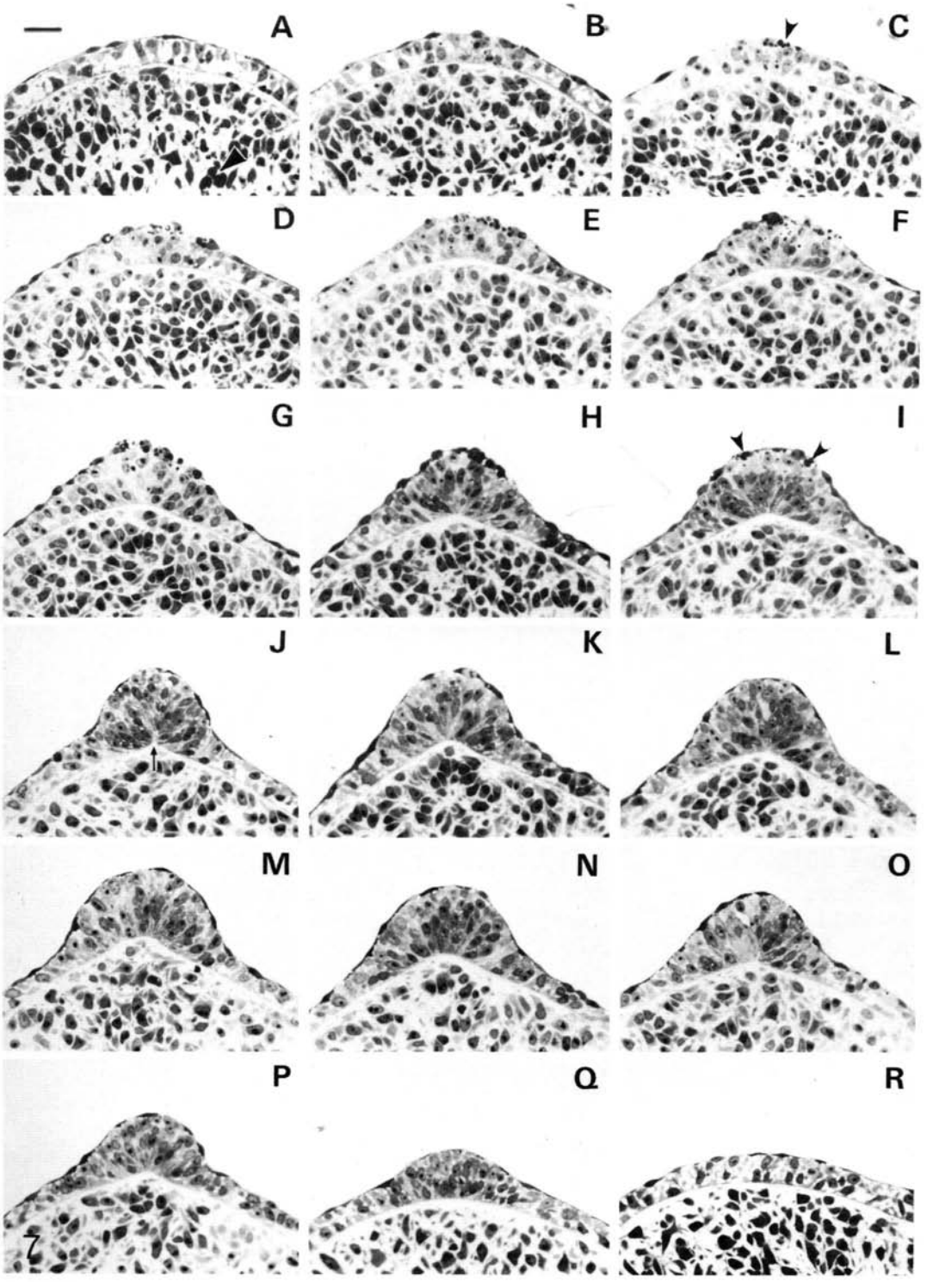

Fig. 7

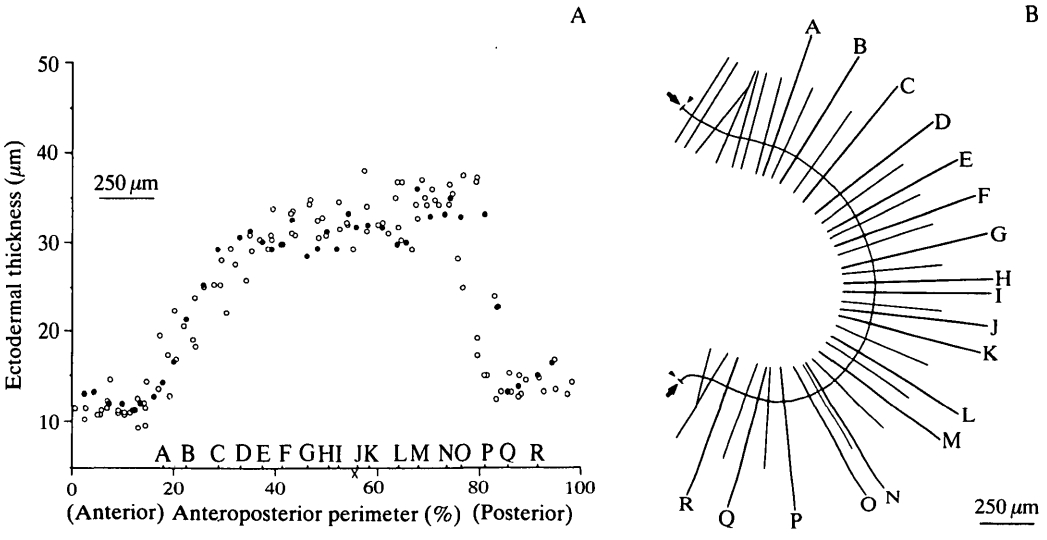

Fig. 8. Stage 23.

(A) The relationship between ectodermal thickness and location (relative to the anteroposterior perimeter) for five wing buds. Solid dots are data from the wing bud pictured in (B). Letters along the abscissa correspond to locations in (B) and to the micrographs in Fig. 9. To determine the position of the axial line, indicated by the X (55·5 % ± 2·0 S.D.), two lines were drawn parallel to each other to approximate the anterior and posterior borders of the wing bud (see Fig. 8B). The axial line was parallel to and midway between these two lines.

(B) Camera-lucida drawing of the wing bud indicated by the solid dots in (A). The curve indicated by the arrows is the outline of the wing bud; the anterior and posterior boundaries of the wing bud are indicated by the arrowheads. Lines intersecting the wing bud outline mark the position of the sections examined for that wing bud. Heavy lines have letters corresponding to those along the abscissa in (A) and to the micrographs in Fig. 9. Scale bars (A and B) represent 250 μm.

Fig. 9. Stage 23. Micrographs of cross-sections of the wing bud at the locations indicated by the corresponding letters in Fig. 8B. Distal mesoderm is covered with apical ectoderm. Dorsal is to the left, ventral to the right. Micrographs are lettered in sequence, (A) being the most anterior (cranial). In addition, the micrographs are paired. For example, (A) and (R) are approximately the same distance from the axial line, as are (B) and (Q), etc. Note the apical ectodermal cell death (C through P, see arrowheads). Mesodermal cell death (anterior necrotic zone) is seen (A, arrowhead). Compare the subectodermal region in (A) and (R). The notch is prominent along most of the thickened region (D through O). Anteroposterior asymmetry of the ridge with respect to the axial line is apparent when comparing (A) through (D) with (O) through (R). Scale bar (A) represents 20 μm.

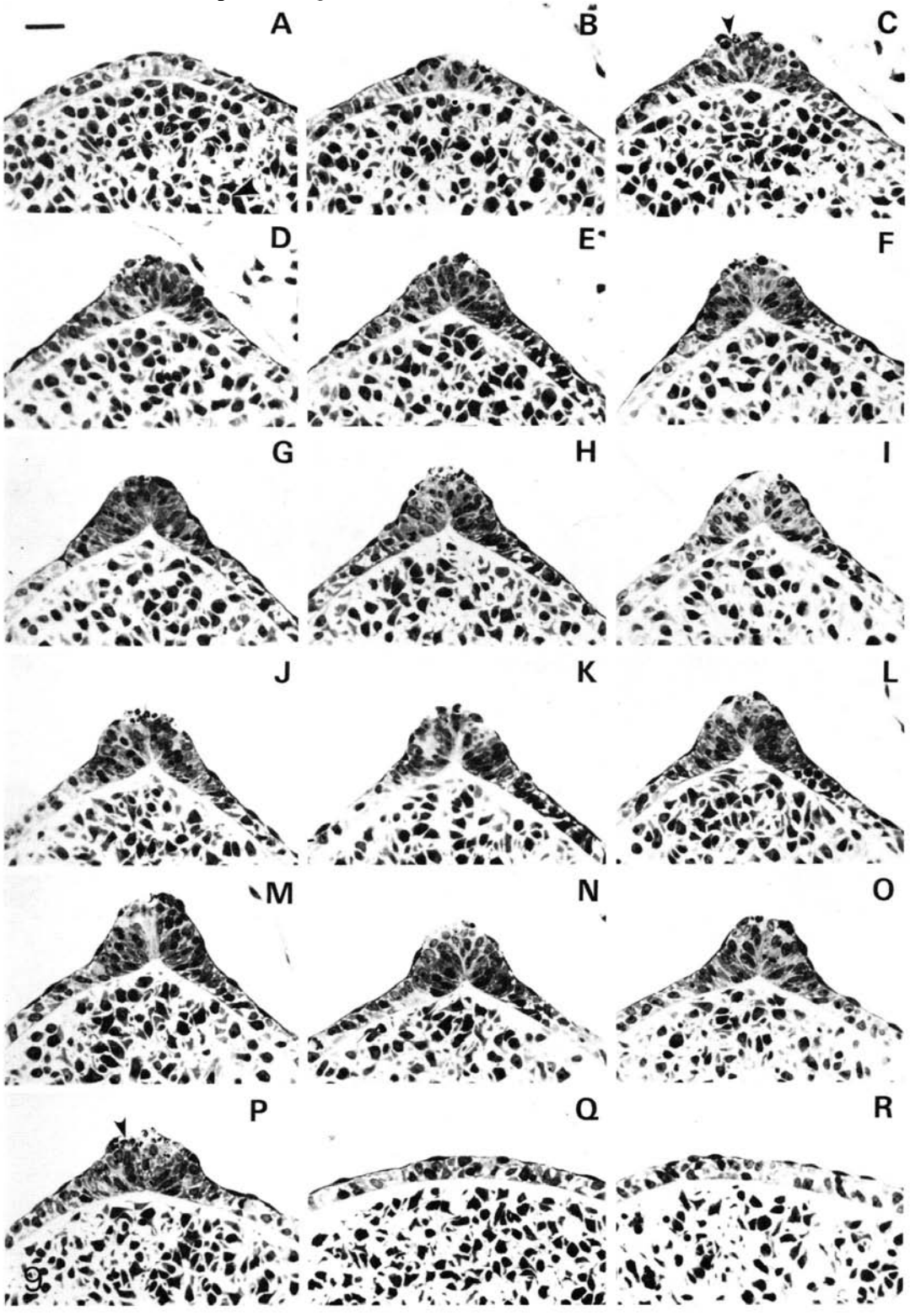

Fig. 9

DISCUSSION

The data presented in this report elucidate several features of apical ectodermal ridge development and morphology which are particularly noteworthy. We have shown that the wing buds in the chick embryo arise without a morphologically identifiable apical ectodermal ridge. In addition we have demonstrated histologically that the wing bud ridge is asymmetric, i.e., by stage 19 the ridge is more prominent posteriorly. We have described the spatial and temporal appearance of a notch in the base of the ridge beginning at stage 20. Finally, we have described an anteroposterior progression of ectodermal cell death, which begins during stage 18 and continues through each of the stages examined.

Early ridge structure and function

Well-developed apical ectodermal ridge in avian species is a pseudostratified columnar epithelium with an overlying periderm (Fallon & Kelley, 1977). In the chick, wing buds are visible as thickenings of the somatopleural mesoderm by stage 17. There are two points worthy of consideration. First, an apical ectodermal ridge is not visible until late stage 18 and the ridge is not a pseudostratified columnar epithelium until stage 20. Second, it is important to recall that mesodermal dependence upon the apical ectoderm prior to stage 20 has been demonstrated both for the proximodistal specification of wing elements (Saunders, 1948; Summerbell, 1974) and for survival of the distal wing bud mesoderm (Rowe, Cairns & Fallon, 1982). Therefore, it becomes necessary to separate pseudostratified columnar morphology and ridge function as defined by ridge removal experiments. In this context, it is evident that little is known about the development of ridge function in the apical ectoderm.

Ridge asymmetry

In his initial report concerning the apical ectodermal ridge, Saunders (1948) noted that the 'greatest thickness of the apical ectoderm is to be found in the posterior half of the bud where its elongation is most rapid' (p. 383). However,

---

Fig. 10. Ectodermal thickness versus relative distance along the anteroposterior perimeter for (A) stage 20, (B) stage 21, and (C) stage 23. Cross-hatched area indicates the portion of the anteroposterior perimeter associated with prospective bone forming areas as calculated from data of Stark & Searls (1973). Stippled area indicates the portion of ridge which displays a groove in the base of the ectoderm. Solid area in (B) and (C) corresponds to the portion of the apical perimeter associated with high polarizing activity as mapped by Summerbell & Honig (1982). Data from individual wing buds have been connected by lines. It is stressed that we do not mean to imply a linearity of ectodermal thickness between points. However, the lines have been included to give a better description of the shape of individual profiles. X marks the location of the axial line (see explanation, Figs 4A and 8A). Scale bars represent 250 μm.

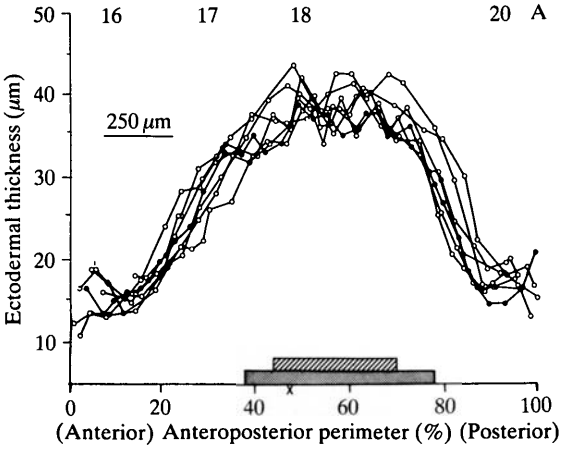
50
16
17
18
20
A
Ectodermal thickness (μm)
40
30
20
10
250 μm
0
20
40
60
80
100
(Anterior) Anteroposterior perimeter (%) (Posterior)

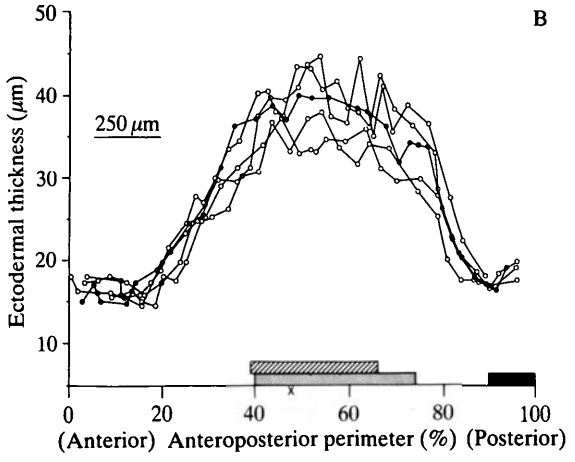
50
B
Ectodermal thickness (μm)
40
30
20
10
250 μm
0
20
40
60
80
100
(Anterior) Anteroposterior perimeter (%) (Posterior)

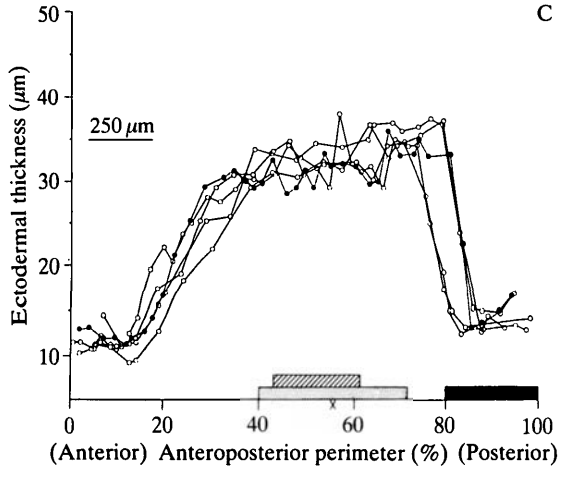
50
C
Ectodermal thickness (μm)
40
30
20
10
250 μm
0
20
40
60
80
100
(Anterior) Anteroposterior perimeter (%) (Posterior)

even at stage 19, before the shape of the wing bud is asymmetric due to its posteriorly directed growth, we have demonstrated that the ridge is thicker at posterior wing bud levels. Data from experiments *in ovo* (e.g., Zwilling, 1956) and *in vitro* (see MacCabe, Leal & Leal, 1983) have been interpreted to mean that apical ridge asymmetry may be a reflection of an asymmetric distribution of mesodermal factors. This possibility needs further investigation.

A specific region of mesoderm called the polarizing zone (zone of polarizing activity; Balcuns, Gasseling & Saunders, 1970) may influence ridge asymmetry in the wing bud. Located along the posterior limb bud border, the polarizing zone has the capacity to induce polarized supernumerary outgrowths when transplanted to other limb sites (Saunders & Gasseling, 1968). The location of tissue with high polarizing activity has been mapped precisely by Summerbell & Honig (1982) (see also MacCabe, Gasseling & Saunders, 1973). By our calculations, using their data, at stage 21 the distal boundary of high polarizing activity is near 90 % of the anteroposterior perimeter. At stage 23, the distal boundary is near 80 % of the anteroposterior perimeter. As seen in Fig. 10, the polarizing zone, indicated by the solid area, is just posterior (proximal) to thick ridge and is always covered with thin ectoderm. At stage 18 (32–33 pairs of somites), even before the ridge is formed, the region of the wing bud with the strongest polarizing activity (opposite somites 19 and 20) is covered with ectoderm thinner than that seen at more anterior wing bud levels (Fig. 1A). Thus, the sharp transition from thick ridge to posterior ectoderm, a major factor in the asymmetric appearance of the ridge *in situ* (Cairns, 1977), is located just anterior (distal) to the polarizing zone. In this context, it is important to point out that not only is the polarizing zone covered with thin ectoderm *in situ*, but when polarizing zone is placed immediately subjacent to thick ridge, the ridge flattens (Gasseling & Saunders, 1964; Saunders & Gasseling, 1968). Therefore, it is possible that the location of the posterior boundary of the wing bud ridge is a result of the influence of the polarizing zone, but this has not been investigated.

Two additional factors may be related to asymmetry in the chick wing bud. First, an anteroposterior progression of cell death is seen in the apical ectoderm. Ectodermal cell death in the chick wing bud has been reported previously, but no reference was found to cell death in the ectoderm of normal wing buds prior to stage 22 (Jurand, 1965; Hinchliffe & Ede, 1967). We have observed cell death in the anterior apical epithelium at late stage 18. Whether the cell death contributes to the morphological asymmetry of the ridge, as suggested by Milaire for the rat and mouse (1977), cannot be determined from the results of this study. Second, the subectodermal space seen along the posterior border of the wing bud after stage 19 may be another reflection of anteroposterior asymmetry. While this observation may be a fixation artifact, it is remarkably consistent under the conditions of this study. The space has been noted previously (see Ede *et al.* 1974 and Sawyer, 1982) and warrants further investigation.

The notch represents a groove in the base of the ridge

The notch in the base of the ectoderm is seen in cross sections through the thickest portions of apical ectodermal ridge beginning at stage 20 (Fig. 10). Because the notch is seen in cross sections from a large extent of the anteroposterior perimeter, it can be considered to represent a groove in the base of the thickest portions of apical ectodermal ridge. The notch in the base of the ridge has been displayed as a prominent feature of ridge morphology in many reports published previously (e.g., see fig. 19 of Saunders, 1948). Jurand (1965) described a 'median line' where the cells of the ridge converge. Tomasek, Mazurkiewiez & Newman (1982), using indirect immunofluorescence, showed an accumulation of fibronectin in the notch in chick wing buds at stages 23, 25 and 28. They also mentioned a deep cleft subjacent to the apical ridge in the duck wing bud. In addition to these avian species, the notch has been seen in the garden lizard (Goel & Mathur, 1977) and the green lizard (Raynaud, Brabet & Adrian, 1979). The notch has not been reported as a feature of mammalian ridges (mouse: Jurand, 1965; human: Kelley, 1973, and Kelley & Fallon, 1976; mammals from several orders: Fallon & Kelley, 1977).

Despite its appearance in the literature as a feature of normal avian ridge morphology, specific references to the notch (groove) are rare. While its significance is unknown, we point out the following correlation. Stark & Searls (1973) constructed maps of the prospective skeletal elements of the wing bud. Using their data to determine the location of these elements relative to the anteroposterior perimeter, a correlation is seen between the groove and the portion of the ridge associated with the laying down of distal wing elements (see Fig. 10). Other maps of the wing bud are in basic agreement with this analysis (see Summerbell, 1979; Hinchliffe, Garcia-Porrero & Gumpel-Pinot, 1981; Rowe & Fallon, 1981).

Ridge thickness

By observing the wing bud *in ovo* with a dissecting microscope, the ridge is seen to be more prominent at stage 23 than at stage 20. However, our data demonstrate that there is a decrease in ridge thickness during this period (Table 1). We believe this apparent discrepancy may be resolved through consideration of two factors. First, a groove begins to develop in the base of the thickest ridge at stage 20. Second, the transition from ridge to adjacent dorsal and ventral ectoderm becomes more pronounced between stage 20 and 23. Our measurements reflect the distance from the base of the ectoderm to its apex as viewed in cross section and not the extent to which the ridge rises above the adjacent limb ectoderm. Thus, the formation of the groove and the rapid transition from dorsal ectoderm to ridge may make the ridge appear to be thicker in gross observations when, in fact, the epithelium itself has become thinner.

We stress that the apical ectodermal ridge is undergoing morphogenetic

changes during stages 20 to 23 and that ectodermal thickness, taken alone, is not adequate for a complete description of ridge morphology. We intend to investigate interactions occurring at the limb bud apex relevant to proximodistal outgrowth in both normal development and under experimental conditions. The study presented here lays the groundwork for these investigations.

This investigation was supported by NIH Grant No. T32HD07118 and NSF Grant No. PCM8205368. We are grateful to R. Auerbach, E. Boutin, J. Carrington, A. Clark, L. Dvorak, R. Fuldner, M. Lanser, J. Pettersen, B. K. Simandl and D. Slautterback for their constructive criticism of this work. Special thanks to B. K. Simandl for expert technical assistance in all aspects of this work. We thank Ms Sue Leonard for typing the manuscript.

REFERENCES

BALCUNS, A., GASSELING, M. T. & SAUNDERS, J. W., JR. (1970). Spatio-temporal distribution of a zone that controls anteroposterior polarity in the limb bud of the chick and other bird embryos. *Amer. Zool.* **10**, 323.

CAIRNS, J. M. (1977). Growth of normal and *talpid*^{2} chick wing buds: An experimental analysis. In *Vertebrate Limb and Somite Morphogenesis* (eds D. A. Ede, J. R. Hinchliffe & M. Balls), pp. 123–137. Cambridge: Cambridge University Press.

CAMOSSO, M. E. & RONCALI, L. (1968). Time sequence of the process of ectodermal ridge thickening and of mesodermal cell proliferation during apical outgrowth of the chick embryo wing bud. *Acta Embryol. Morph. exp.* **10**, 247–263.

EDE, D. A., BELLAIRS, R. & BANCROFT, M. (1974). A scanning electron microscope study of the early limb-bud in normal and *talpid*^{3} mutant chick embryos. *J. Embryol. exp. Morph.* **31**, 761–785.

FALLON, J. F. & KELLEY, R. O. (1977). Ultrastructural analysis of the apical ectodermal ridge during vertebrate limb morphogenesis. II. Gap junctions as distinctive ridge structures common to birds and mammals. *J. Embryol. exp. Morph.* **41**, 223–232.

GASSELING, M. T. & SAUNDERS, J. W., JR. (1964). Effect of the "Posterior Necrotic Zone" of the early chick wing bud on the pattern and symmetry of limb outgrowth. *Amer. Zool.* **4**, 303–304.

GOEL, S. C. & MATHUR, J. K. (1977). Morphogenesis in reptilian limbs. In *Vertebrate Limb and Somite Morphogenesis* (eds D. A. Ede, J. R. Hinchliffe & M. Balls), pp. 387–404. Cambridge: Cambridge University Press.

HAMBURGER, V. & HAMILTON, H. L. (1951). A series of normal stages in the development of the chick embryo. *J. Morph.* **88**, 49–92.

HINCHLIFFE, J. R. & EDE, D. A. (1967). Limb development in the polydactylous talpid^3 mutant of the fowl. *J. Embryol. exp. Morph.* **17**, 385–404.

HINCHLIFFE, J. R., GARCIA-PORRERO, J. A. & GUMPEL-PINOT, M. (1981). The role of the zone of polarizing activity in controlling the differentiation of the apical mesenchyme of the chick wing-bud: histochemical techniques in the analysis of a developmental problem. *Histochem. J.* **13**, 643–658.

JURAND, A. (1965). Ultrastructural aspects of early development of the fore-limb buds in the chick and the mouse. *Proc. Roy. Soc. B* **162**, 387–405.

KELLEY, R. O. (1973). Fine structure of the apical rim-mesenchyme complex during limb morphogenesis in man. *J. Embryol. exp. Morph.* **29**, 117–131.

KELLEY, R. O. & FALLON, J. F. (1976). Ultrastructural analysis of the apical ectodermal ridge during vertebrate limb morphogenesis. I. The human forelimb with special reference to gap junctions. *Devl Biol.* **51**, 241–256.

KIENY, M. (1968). Variation de la capacité inductrice du mésoderme et de la competence de l'ectoderme au cours de l'induction primaire du bourgeon de membre, chez l'embryon de poulet. *Archs Anat. microsc. Morp. exp.* **57**, 401–418.

MacCabe, A. B., Gasseling, M. T. & Saunders, J. W., Jr. (1973). Spatiotemporal distribution of mechanisms that control outgrowth and anteroposterior polarization of the limb bud in the chick embryo. *Mech. Aging Develop.* **2**, 1–12.

MacCabe, J. A., Leal, K. W. & Leal, C. W. (1983). The control of axial polarity: A. A low molecular weight morphogen affecting the ectodermal ridge. B. Ectodermal control of the dorsoventral axis. In *Limb Development and Regeneration, Part A* (eds J. F. Fallon & A. I. Caplan), pp. 237–244. New York: Alan R. Liss, Inc.

Milaire, J. (1977). Histochemical expression of morphogenetic gradients during limb morphogenesis (with particular reference to mammalian embryos). *Birth Defects* **13**, 37–67.

Raynaud, A., Brabet, J. & Adrian, M. (1979). Étude ultrastructurale comparative de la crête apicale des ébauches des membres des embryons d'orvet (*Anguis fragilis* L.) et des embryons de lézard vert (*Lacerta viridis* Laur.). *Archs Anat. microsc. Morp. exp.* **68**, 301–332.

Rowe, D. A., Cairns, J. M. & Fallon, J. F. (1982). Spatial and temporal patterns of cell death in limb bud mesoderm after apical ectodermal ridge removal. *Devl Biol.* **93**, 83–91.

Rowe, D. A. & Fallon, J. F. (1981). The effect of removing posterior apical ectodermal ridge of the chick wing and leg on pattern formation. *J. Embryol. exp. Morph.* **65** (suppl.), 309–325.

Rowe, D. A. & Fallon, J. F. (1982). The proximodistal determination of skeletal parts in the developing chick leg. *J. Embryol. exp. Morph.* **68**, 1–7.

Saunders, J. W., Jr. (1948). The proximo-distal sequence of origin of the parts of the chick wing and the role of the ectoderm. *J. exp. Zool.* **108**, 363–403.

Saunders, J. W., Jr. (1977). The experimental analysis of chick limb bud development. In *Vertebrate Limb and Somite Morphogenesis* (eds D. A. Ede, J. R. Hinchliffe & M. Balls), pp. 1–24. Cambridge: Cambridge University Press.

Saunders, J. W., Jr. & Gasseling, M. T. (1968). Ectodermal-mesenchymal interactions in the origin of limb symmetry. In *Epithelial-Mesenchymal Interactions* (eds R. Fleischmajer & R. Billingham), pp. 78–97. Baltimore: Williams and Wilkins.

Saunders, J. W. Jr. & Gasseling, M. T. & Saunders, L. C. (1962). Cellular death in morphogenesis of the avian wing. *Devl Biol.* **5**, 147–178.

Saunders, J. W., Jr. & Reuss, C. (1974). Inductive and axial properties of prospective wing-bud mesoderm in the chick embryo. *Devl Biol.* **38**, 41–50.

Sawyer, L. M. (1982). Fine structural analysis of limb development in the wingless mutant chick embryo. *J. Embryol. exp. Morph.* **68**, 69–86.

Stark, R. J. & Searls, R. L. (1973). A description of chick wing bud development and a model of limb morphogenesis. *Devl Biol.* **33**, 138–153.

Summerbell, D. (1974). A quantitative analysis of the effect of excision of the AER from the chick limb-bud. *J. Embryol. exp. Morph.* **32**, 651–660.

Summerbell, D. (1979). The zone of polarizing activity: evidence for a role in normal chick limb morphogenesis. *J. Embryol. exp. Morph.* **50**, 217–233.

Summerbell, D. & Honig, L. S. (1982). The control of pattern across the antero-posterior axis of the chick limb bud by a unique signalling region. *Amer. Zool.* **22**, 105–116.

Tomasek, J. J., Mazurkiewicz, J. E. & Newman, S. A. (1982). Nonuniform distribution of fibronectin during avian limb development. *Devl Biol.* **90**, 118–126.

Zwilling, E. (1956). Interaction between limb bud ectoderm and mesoderm in the chick embryo. II. Experimental limb duplication. *J. exp. Zool.* **132**, 173–187.

Zwilling, E. (1961). Limb morphogenesis. *Adv. Morphogen.* **1**, 301–330.

(Accepted 23 November 1983)